Real-time dynamic movement of caveolin-1 during smooth muscle contraction of human colon and aged rat colon transfected with caveolin-1 cDNA

Sita Somara, Daniela Bashllari, Robert R. Gilmont, and Khalil N. Bitar

Gastrointestinal Molecular Motors Laboratory, Department of Pediatrics, Gastroenterology, University of Michigan Medical Center, Ann Arbor, Michigan

Somara S, Bashllari D, Gilmont RR, Bitar KN. Real-time dynamic movement of caveolin-1 during smooth muscle contraction of human colon and aged rat colon transfected with caveolin-1 cDNA. *Am J Physiol Gastrointest Liver Physiol* 300: G1022–G1032, 2011. First published March 3, 2011; doi:10.1152/ajpgi.00301.2010.— Caveolin-1 (cav-1) plays a key role in PKC-α and RhoA signaling pathways during acetylcholine (ACh)-induced contraction of colonic smooth muscle cells (CSMC). Aged rat CSMC showed sluggish contractility, concomitant with reduced expression of cav-1 with an associated reduction in activation of PKC-α and RhoA signaling pathway. Real-time monitoring of live human CSMC transfected with yellow fluorescent protein-tagged wild-type caveolin 1 cDNA (YFP-wt-cav-1) cDNA in the present study suggests that cav-1 cycles within and along the membrane in a synchronized, highly organized cytoskeletal path. These studies provide, for the first time, the advantages of real-time monitoring of the dynamic movement of caveolin in living cells. Rapid movement of cav-1 in response to ACh suggests its dynamic role in CSMC contraction. Human CSMC transfected with YFP-ΔTFT-cav-1 dominant negative cDNA show fluorescence in the cytosol of the CSMC and no movement of fluorescent cav-1 in response to ACh mimicking the response shown by aged rat CSMC. Transfection of CSMC from aged rat with YFP-wt-cav-1 cDNA restored the physiological contractile response to ACh as well as the dynamic movement of cav-1 along the organized cytoskeletal path observed in normal adult CSMC. To study the force generation by CSMC, three-dimensional colonic rings were bioengineered. Colonic bioengineered rings from aged CSMC showed reduced force generation compared with colonic bioengineered rings from adult CSMC. Colonic bioengineered rings from aged CSMC transfected with wt-cav-1 cDNA showed force generation similar to colonic bioengineered rings from adult rat CSMC. The data suggest that contraction in CSMC is dependent on cav-1 reorganization dynamics, which restores the physiological contractile response in aged CSMC. We hypothesize that dynamic movement of cav-1 is essential for physiological contractile response of colonic smooth muscle.

signal transduction; three-dimensional bioengineered colonic rings; force generation; age-related sluggish motility

AGING AFFECTS THE PHYSIOLOGICAL functions of different tissues and organs. The effect of aging on gastrointestinal motility is limited to few clinical studies on human subjects. There is considerable evidence that incidences of dysphasia and constipation increase dramatically with age (9). The major age-related gastrointestinal disorders are associated with impairment in colonic motility that dictates impaired smooth muscle contraction (7, 9, 32, 50). Recent studies from our laboratory have shown the effect of aging on the cellular mechanisms of signal transduction and association of contractile proteins in colonic smooth muscle cells (CSMC) of the aged rats (47).

Contraction in colonic smooth muscle is maintained with a balance between the activities of myosin light chain kinase (MLCK) and myosin light chain phosphatase (MLCP) that regulate phosphorylation of myosin light chain (MLC$_{20}$) (38). Different signal transduction mechanisms regulate smooth muscle contraction by modulating activities of either MLCK or MLCP. The initial contractile response (30 s) is dependent on MLCK-mediated MLC$_{20}$ phosphorylation, whereas the sustained contractile response (4 min) is associated with maintenance of MLC$_{20}$ phosphorylation mediated by inhibition of MLCP (10). MLCP activity is regulated by PKC and RhoA/ROCK pathways in smooth muscle (38). MLCP is a trimeric enzyme consisting of myosin phosphatase-targeting subunit (MYPT), catalytic subunit (PP1c), and a small subunit of unclear function (22, 25). Activation of the RhoA/ROCK pathway results in phosphorylation of MYPT and inhibition of MLCP activity. Activation of the PKC pathway induces phosphorylation of CPI-17, which is a potent inhibitor of PP1c and also results in the inhibition of MLCP activity (24). Agonist-induced contraction of CSMC is associated with translocation and sequestration of RhoA and PKC-α to caveolae of the membrane (39, 49), where they activate RhoA/ROCK and PKC pathways, respectively. CSMC from aged rat showed reduced shortening of cell length concomitant to reduced expression of caveolin-1 (cav-1). CSMC from aged rat showed reduction in phosphorylation of CPI-17 (a substrate for PKC), and of MYPT, implying impairment of both PKC-α and RhoA pathways (47). Decreased phosphorylation of CPI-17 and of MYPT leads to MLCP activation resulting in dephosphorylation of MLC$_{20}$. Age-related reduction in cav-1 expression leads to inhibition or reduction in the activation of RhoA/ROCK and PKC pathways due to impaired translocation of RhoA and PKC-α to caveolae in the membrane (47).

Caveolae are flask-shaped membrane invaginations that are abundant in endothelial cells, adipocytes, cardiac myocytes, and smooth muscle cells (SMCs) (16, 49). Caveolae are characterized by high cholesterol-sphingolipid content and the caveolin proteins (2). The caveolin gene family consists of three members: cav-1, caveolin-2 (cav-2), and caveolin-3 (cav-3), which represent the functional assembly units of caveolae (37, 41, 45). Taggart et al. (49) reported that PKC-α exhibited a stimulus-dependent translocation to the plasma membrane of SMCs, where they may interact with caveolins in caveolae. Cav-1 also has been found to interact with a wide variety of signal transducing molecules, including PKC-α and RhoA (5, 17). Previous studies from our laboratory have shown interaction of cav-1 with PKC-α and RhoA in the particulate fraction of CSMC, in response to acetylcholine (ACh), suggesting that contraction is associated with sequestration of PKC-α and RhoA in caveolae (47). In cardiac myocytes, specific β-adrenergic receptor subtypes and adenylate cyclase are localized to

Address for reprint requests and other correspondence: K. N. Bitar, Univ. of Michigan Medical School, 1150 W. Medical Center Dr., MSRB I, Rm. A520, Ann Arbor, MI 48109-0658 (e-mail: bitar@umich.edu).

caveolae (17) and various PKC isoforms translocate to caveolae following activation (35). In contrast, activated adenosine receptors translocate out of caveolae (29). There is increasing evidence that caveolae may contain key components for Ca^{2+} handling and may serve as initiation sites for Ca^{2+} sparks in cardiac and smooth muscle myocytes (28, 31). Thus caveolae are essential modulators of signal transduction pathways.

Expression of cav-1 was affected by age since there was significant decrease in cav-1 expression in aged rats, suggesting that regulation of transmembrane signaling by caveolin may differ in aging (27, 47). The interaction between cav-1 and the signaling molecules is mediated via a membrane-proximal region of caveolin, caveolin-scaffolding domain (CSD: residue 82–101) (13). Specific G protein-coupled and tyrosine kinase receptors, as well as downstream signaling intermediaries, are caveolae associated (40, 44). CSD interacts with a variety of signaling molecules including G protein-α subunits, MAPK, endothelial nitric oxide synthase, H-ras, Src-family tyrosine kinases, PKC isoforms, EGF receptor, Neu, eNOS, and RhoA (36, 49). Multiple cell signaling pathways converge through interactions with caveolin to regulate excitation-contraction coupling in smooth muscle. Sequestration in caveolae has been suggested to facilitate receptor signaling and has been proposed to play a key role in receptor internalization. The downregulation of cav-1 affects all the associated signaling pathways (12, 13). Transfection of CSMC with dominant negative (DN) cav-1 (YFP-ΔTFT-cav-1:mutant CSD, where TFT mutant is deletion of amino acids threonine-phenylalanine-threonine: 91–93 aa in the scaffolding domain) cDNA inhibits PKC-α translocation concomitant with inhibition of PKC-α association with cav-1 in rabbit CSMC (47). This confirmed the concept that cav-1 regulates the integration of extracellular contractile stimuli and downstream intracellular effectors in smooth muscle (49). Disruption of caveolae by cholesterol depletion in denuded caudal arteries from the rat has shown impairment in serotonin (5-HT$_{2A}$) as well as endothelin-1 (ET-1) receptor signaling. Furthermore, restoration of caveolae by cholesterol replenishment recovered signaling from both receptors (3, 4, 14). In ureteric muscle, cholesterol depletion affected phasic but not tonic contraction, suggesting that caveolae-related signaling regulates specific steps in excitation-contraction coupling (1).

Here, for the first time, we present the real-time monitoring of cav-1 dynamics in live CSMC and we correlate it with the real-time force generation in bioengineered tissue constructs of CSMC. The real-time monitoring of fluorescence provides us the advantage of studying the dynamic movement of caveolin in live cells. Earlier work from our laboratory has shown the essential role of cav-1 in signal transduction during contraction of CSMC (47). CSMC overexpressing DN cav-1 exhibited impaired signal transduction as observed by inhibited translocation of PKC-α and RhoA. Investigations were carried out to examine whether levels of expression correlate to the dynamic movement of cav-1 and whether dynamic movement of cav-1 is essential for contractile response in CSMC. Here, we elaborate the dynamic nature of caveolae in normal adult CSMC and its impairment due to aging. Three-dimensional bioengineered rings from CSMC of human, adult, and aged rats (23) were used to study the physiological contractile response to ACh.

Transfection of aged CSMC with cav-1 reinstated *1*) overexpression of cav-1 as seen under confocal microscopy; this was confirmed in *2*) reinstatement of lipid raft microdomains, *3*) reinstatement of increased ACh-induced dynamic, cycling movement of cav-1 along membrane as monitored in real time, and *4*) reinstatement of force generation in colon rings bioengineered from aged CSMC transfected with cav-1. The data suggest that dynamic movement of cav-1 is a crucial requirement for physiological contractile response of smooth muscle from colon. Furthermore, we propose that restoration of contractile response upon ectopic expression of cav-1 emphasizes the restoration of cav-1 dynamics that reinstates contractile response in smooth muscle from aged.

MATERIALS AND METHODS

Materials

G-418, penicillin/streptomycin, fetal bovine serum, and Dulbecco's modified Eagle's medium (DMEM) were from GIBCO BRL, Grand Island, NY. Collagenase type II was from Worthington, Lakewood, NJ. Cav-1 antibody was purchased from BD Biosciences, Secondary antibody conjugated with fluorescence was purchased from Jackson ImmunoResearch Laboratories. Aged (28–33 mo) rats were obtained National Institute on Aging, Bethesda, MD and adult (12–18 mo) were obtained from Harlan Laboratories, Madison, WI.

Isolation of CSMCs from Human Sigmoid Colon and Adult and Aged Rat Colon

SMCs of human sigmoid colon (IRB approval no. 1991-0297 obtained from National Disease Research Interchange) and adult and aged rat colon were isolated as described previously (5). Briefly, circular smooth muscle layer from the distal colon was removed by sharp dissection and digested with collagenase to yield isolated SMCs. The tissue was incubated for two successive 1-h periods at 31°C in 15 ml HEPES (pH 7.4) (in mM): 115 NaCl, 5.7 KCl, 2.0 KH$_2$PO$_4$, 24.6 HEPES, 1.9 CaCl$_2$, 0.6 MgCl$_2$, and 5.6 glucose, containing 0.1% (wt/vol) collagenase (150 U/mg, Worthington CLS type II), 0.01 (wt/vol) soybean trypsin inhibitor, and 0.184 (wt/vol) DMEM. After the end of the second enzymatic incubation period, the medium was filtered through 300-μm Nitex. The partially digested tissue left on the filter was washed four times with 10 ml of collagenase-free buffer solution. Tissue was then transferred into 15 ml of fresh collagenase-free buffer solution, and cells were gently dispersed. After a hemocytometric cell count, the harvested cells were resuspended in collagenase-free HEPES buffer (pH 7.4) and plated in growth media.

Transfection of CSMCs

Isolated CSMC were transfected either with YFP-tagged wild-type caveolin 1 cDNA (YFP-wt-cav-1) or with mutant YFP-ΔTFT-cav-1 cDNA (DN cav-1). Transfections were carried out using Qiagen Effectene transfection kit. Briefly, confluent CSMCs were passaged on the day before transfection. Cells were washed twice with PBS. The cDNA was diluted with Buffer EC and mixed with enhancer and incubated at room temperature (RT) for 5 min. The DNA-enhancer mixture was well mixed with Effectene transfection reagent and incubated at RT for 10 min. The transfection complex was then mixed with cell culture medium and overlaid on the cells. After 2 days of transfection, the cells were selected with G418 (400 μg/ml). The cells were grown on coverslips for microscopy studies.

Lipid Raft Preparation

Detergent-free purification of caveolae-enriched membrane fractions was carried out following the method described by Lisanti et al. (30) with slight modifications. Briefly, rabbit CSMCs were washed twice with cold 1$\times$ PBS (pH 7.4), and scraped into 500 mM sodium carbonate (pH 11, Sigma) plus caveolin-enriched membrane (CEM) buffer [25 mM 4-morpholineethanesulfonic acid (MES), 150 mM NaCl, 1 mM PMSF, 10 mg/ml aprotinin, and 10 mg/ml leupeptin].

Cells were homogenized and sonicated for 20–30 s, and the sample (3 ml) was adjusted to 40% sucrose by the addition of 3 ml 80% sucrose in CEM buffer before placement at the bottom of an ultracentrifuge tube (Beckman Coulter, Hayward, CA). Two milliliters each of 25, 15, and 5% sucrose in 250 mM sodium carbonate (pH 11) plus CEM buffer was then sequentially layered above. The discontinuous gradient was centrifuged at 36,000 rpm for 22 h with a Beckman SW50.1 rotor, after which 12 1-ml fractions were collected from the top to bottom of the tube. The pellet fraction (fraction 12) was separately sonicated in 12 ml MES buffer. Equal volume aliquots were analyzed by SDS-PAGE and immunoblotting.

SDS-PAGE and Immunoblotting

For one-dimensional SDS-PAGE, the samples were mixed in an equal volume of 2× sample buffer [50 mM Tris, 10% (vol/vol) glycerol, 2% (wt/vol) SDS, and 0.1% (wt/vol) bromophenol blue, pH 6.8]. The proteins were separated by 10 or 12% SDS-PAGE and transferred onto polyvinylidene difluoride (PVDF) membranes. The PVDF membrane was then blocked with 5% nonfat dry milk for 1 h. Following blocking, the membrane was incubated in an appropriate dilution of primary antibody in 5% nonfat dry milk in TBST (Tris-buffered saline-Tween 20) for 1 h. The membrane was washed thrice with Tris-buffered saline to remove unbound primary antibody for 15 min each wash at room temperature. The membrane was then incubated in an appropriate dilution of secondary antibody in 5% nonfat dry milk in TBST for 1 h at room temperature. The membrane was washed thrice with TBST for 15 min each wash at room temperature to remove unbound secondary antibody. The membrane was then incubated with ECL reagent for 1 min. The proteins were detected on the membrane by immediately exposing the membrane to the film for 30 s and 1 min.

Immunofluorescence

Coverslips were autoclaved and placed in six-well plates. CSMC were plated and incubated for 30 h. CSMC on the coverslips were exposed to ACh (30 s and 4 min). CSMC with no exposure were used as control. Reaction was stopped by adding 3.5% formaldehyde in PBS to coverslips for 10 min. Following the removal of formaldehyde, the cells were washed twice with 100 mM glycine buffer pH 7.4 for 5 min followed by washing with PBS. One milliliter of permeabilization solution (0.5% CHAPS in 1× PBS) containing 0.15% Triton X-100/5% goat serum was added to each coverslip for 10 min. After removing the permeabilization/goat serum solution, primary antibody (mouse anti-cav-1: diluted in 0.5% CHAPS with 10% goat serum in 1× PBS) was added and incubated overnight. Coverslips were then washed thrice with PBS for 10 min each time. Then secondary antibody conjugated with fluorescence (FITC-AffiniPure Fab fragment goat anti-mouse IgG) was added and incubated for 1 h. Coverslips were then washed thrice with PBS for 10 min each time and were mounted on the slides with mounting media.

Confocal Microscopy

Transfected CSMC was grown on a coverslip. The movement of cav-1 in response to ACh was monitored in real time under confocal microscopy. Images of transfected cells displaying fluorescent signals were acquired on an Olympus FluoView 500 confocal microscope with a ×100 1.35 numerical aperture oil objective. Exposure times were adjusted so that the maximal pixel intensities were at least half saturation. Images were obtained by taking a series of stacks every 0.5 mm through the cell (generally 3–5 mm) and combining the images into a composite stack. Real-time movement of YFP-cav-1 was monitored in response to ACh by scanning a desired square-micrometer area. Contrast and brightness of composite images were further optimized with Adobe Photoshop CS version 8.0 (Adobe Systems, San Jose, CA) on an Optiplex GX280 PC (Dell, Round Rock, TX). Images were analyzed with ImageJ software (NIH, Bethesda, MD).

The data were statistically developed by analyzing the region of interest using stack difference tool of ImageJ software. Calculating the mean of the movement of all the fluorescence particles and finding the difference between the mean movement before and after ACh stimulation between each frame gives the value of real movement, which is then expressed as percentage. Statistics were performed with ImageJ Stack difference mean analysis and Prism software from GraphPad Prism Software (San Diego, CA).

FRAP

Fluorescence recovery after photobleaching (FRAP) was used to determine whether cav-1 protein was able to move within the plasma membrane. Forty-eight hours after transfection, glass coverslips carrying cells were inserted into a live-cell imaging Quick Change chamber with a heated base (37°C). A prebleach image was acquired at a resolution of 512 × 512 pixels at 3% laser intensity before bleaching a region at 100% laser intensity for 15 s. Recovery was measured by obtaining 512 × 512 images at 3% laser intensity for the indicated times. A single focal plane of 0.5–1 μm z-resolution was imaged with a large confocal aperture to minimize drift. After subtracting the background fluorescence, the recovery of the bleached region was normalized to both the initial region intensity relative to whole-cell intensity and to the photobleaching of sample during recovery. Total photobleaching of sample was generally less than 15% over the entire period of recovery. Recovery kinetics was determined with a single exponential fit of the average data: $y = A [1e (\tau \times T)] + c$, in which A is amplitude, T is time, τ is the time constant, and c is the constant representing the relative fluorescence immediately post-bleach.

In Vitro Three-Dimensional CSMC Tissue Model Bioengineered from CSMC of Human and Adult and Aged Rat

Primary CSMC from human and adult and aged rat were isolated as described previously (8) and cultured in 75-cm² flasks. Sylgard-coated culture plates (35 mm) with Sylgard post for bioengineering were prepared as described previously (23). Once confluent, cells (~100 K) were seeded onto these culture plates containing a loose fibrin gel, where they proliferated to confluence. As cells proliferated, they shrank the fibrin gel, contracting it toward the center of the culture dish around a 5-mm-diameter Sylgard post (23). Cells migrated and self-assembled along the line of force until they formed a parallel array of cells. Tissues were considered "formed" when a three-dimensional cylindrical tube of colonic smooth muscle tissue contracted around the Sylgard mold (23). All fibrin constructs seeded with CSMC were fully formed within 5–10 days after cell seeding. The resulting colonic bioengineered ring constructs remained stable in culture and were experimentally tested.

Measurement of Contractile Properties and Force Generation in Bioengineered Colon Constructs

The protocol for measuring force generation of engineered muscle constructs was adapted from previous work. Briefly, colonic bioengineered rings were separated from their molds with forceps, and the minimum ring diameter was measured by using a calibrated eyepiece and a ×5 or ×10 objective lens on an inverted microscope (Axiovert 25; Zeiss, Thornwood, NY). The dish was placed on a heated aluminum platform that was maintained at a temperature of 37°C until the testing was complete. For measurements of force generation, one end of the colonic bioengineered ring was anchored by a stainless steel pin (10 mm × 0.1 mm diameter) to the Sylgard substrate, and another stainless steel pin was bent in the shape of a hook and attached by canning wax to an optical force transducer with a resolution of 1.4 μN and a range of 2 mN. Spontaneous basal tone of colonic bioengineered ring was measured by stretching the tissue (10%) with a three-axis micromanipulator, followed by a period of equilibrium (between 20 and 60 min),

when the colonic bioengineered ring stabilized, resulting in the establishment of a new stable baseline of tension (6, 19).

Testing Protocol

Protocols were designed to confirm that bioengineered colonic rings exhibited parameters similar to those of physiologically functional colon. Bioengineered colonic rings were stretched 10% of their resting length with a three-axis micromanipulator and were allowed to sit for 20–30 min to reestablish a stable baseline. The development of basal tone was analyzed. Bioengineered colonic rings were treated with ACh (10^{-7} M) to study force generation.

RESULTS

Dynamic Organization of Cav-1

Organization of cav-1 in relaxed and contracted human CSMC. Human CSMC were successfully transfected with YFP-wt-cav-1 cDNA. Cav-1 expression was characterized by even cellular distribution with punctuate appearance. Following ACh treatment, reorganization of YFP-wt-cav-1 protein to the distal cell surfaces was observed. Fluorescence was observed in organized form that ran along the length of the cell with denser at the rounded tip of the cell as the CSMC contracted (Fig. 1). This indicated a dynamic movement of cav-1 in response to ACh (0.1 μM). It is unclear whether cav-1 followed a particular path or a preferred localization for organization. Further investigations were carried out to monitor the real-time movement of cav-1 in live CSMC to study the dynamic movement of cav-1 resulting in its reorganization.

Real-time monitoring of dynamic movement of cav-1 in live human CSMC. Dynamic movement of cav-1 was monitored in real time in the human CSMC transfected with YFP-wt-cav-1 cDNA (Fig. 2, *A* and *B*). In human CSMC transfected with YFP-wt-cav-1 cDNA, a rapid cyclic movement of fluorescent cav-1 was observed on the membrane in response to ACh (0.1 μM) stimulation (Fig. 2*C*). The movement was synchronized and organized along the whole length of the cell with characteristic rapid cycling of cav-1 along the membrane. The rapidity of the movement and organization of cav-1 during contraction was further studied by FRAP analysis.

FRAP. FRAP was used to track the movement of cav-1 protein within a membrane of human CSMC. Forty-eight hours after transfection, glass coverslips carrying cells were placed into a live-cell imaging Quick Change chamber with a heated base. Using a 3% laser, the fluorescence was bleached for 15 s as described in the protocols. Dynamic movement of cav-1 was analyzed by measuring the recovery of fluorescence for indicated times (Fig. 3*A*). A single focal plane of 0.5–1 μm *z*-resolution was imaged with a large confocal aperture to minimize the effect of drift. After background fluorescence subtraction, recovery of the bleached region was normalized both to the initial region intensity relative to whole-cell intensity and to the photobleaching of sample during recovery. Total photobleaching was generally less than 15% over the entire period of recovery. Recovery kinetics was determined with a single exponential fit of the average data: $y = A [1e (\tau \times T)] + c$. Movement of cav-1 was tracked with FRAP, both in control human CSMC and in human CSMC treated with ACh (0.1 μM). The relative mean fluorescence in the region vs. time was then plotted (Fig. 3*B*). The graph suggests that a significantly higher percent recovery with fast mobility was observed in the bleached section of the CSMC treated with ACh compared with control CSMC (Fig. 3, *C–F*).

Force generation by colonic bioengineered rings constructed from human CSMC. For the first time, three-dimensional colonic bioengineered rings were constructed successfully from human CSMC, to study the physiological force generation response of CSMC to contractile agonists. Colonic bioengineered rings are distinct from the rings bioengineered from SMC isolated from the internal anal sphincter (IAS) since IAS bioengineered rings exhibit spontaneous, oscillatory, rhythmic contractions at rest (46). Colonic bioengineered rings mimic similar patterns of contractions that occur in circular muscle in vivo. Colonic bioengineered rings were stretched ~10% and allowed to equilibrate before being stimulated with ACh (0.1 μM). An initial response was observed within 1 s of ACh (0.1 μM) addition. The force generated by human colonic bioengineered rings exhibited an initial rapid rise followed by sustained force generation (Fig. 4).
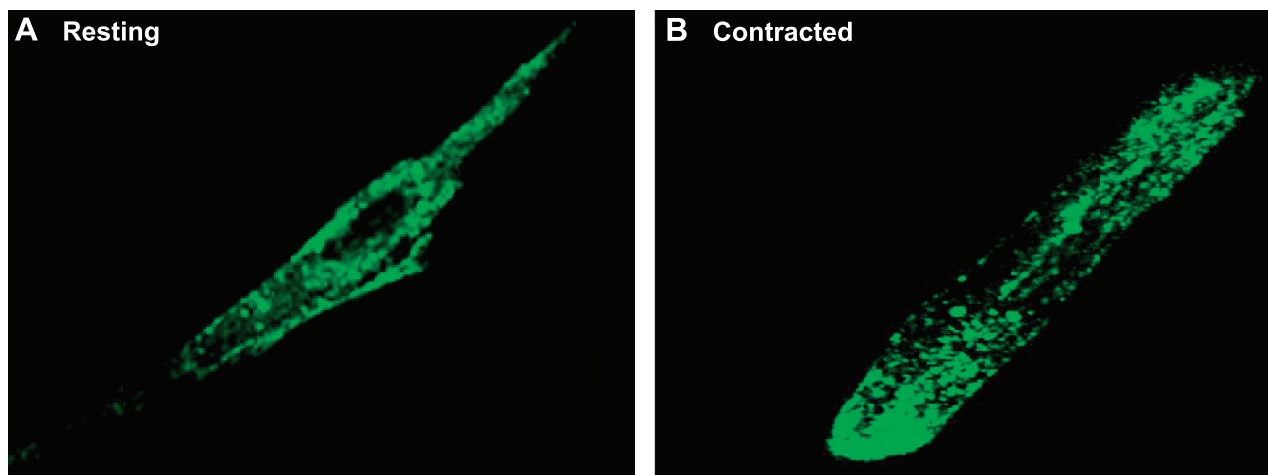

Fig. 1. Human colonic smooth muscle cells (CSMC) were successfully transfected with YFP-wt-cav-1 cDNA (YFP, yellow fluorescent protein; wt, wild-type; cav-1, caveolin-1). Ectopic expression of YFP-cav-1 was characterized by an even cellular distribution of fluorescence with punctuate appearance. Dynamic cyclic movement of YFP-tagged cav-1 protein to the membrane with preferential relocalization of fluorescent YFP-wt-cav-1 to the distal cell surfaces was observed in response to acetylcholine (ACh) treatment.
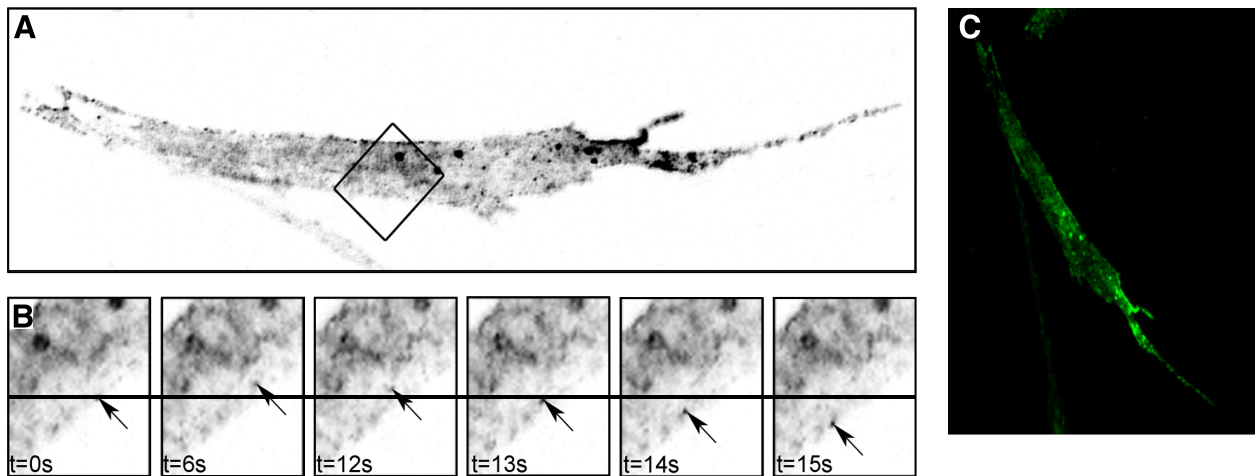
Fig. 2. Active and dynamic movement of cav-1 was monitored in real time in human CSMC transfected with YFP-wt-cav-1 cDNA under confocal microscope (*A* and *B*). A rapid cyclic movement of fluorescent cav-1 was observed on the membrane in response to ACh stimulation (*C*). The dynamic movement of cav-1 was synchronized and organized along the whole length of the cell characterized by rapid cycling of cav-1 along the membrane.

Cav-1 in Aging

Previous studies have shown that expression of cav-1 protein is diminished with aging (47). Reduced expression of cav-1 can impair the downstream functionality of caveolae. Ectopic expression of cav-1 in aged CSMC has restored the contractile response to ACh by restoring the phosphorylation and associ-ations of thin-filament regulatory proteins (47). Investigations were done to examine whether the dynamics of cav-1 were restored by overexpressing cav-1 in aged CSMC.

Expression of cav-1. Caveolin plays a key role in signal transduction by directly binding to and regulating the function of molecules involved in transmembrane signaling, suggesting that the amount of caveolin within cells may be an important
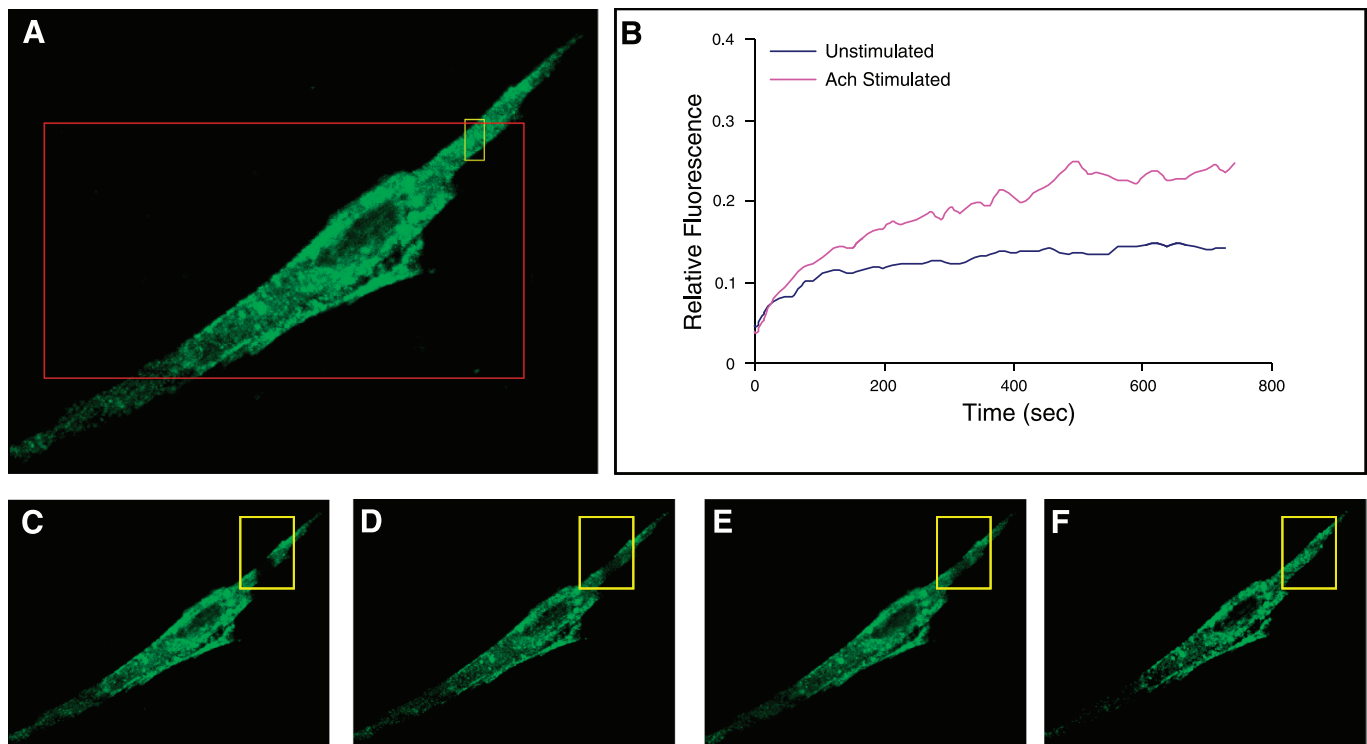
FRAP: Confocal Microscopy

Fig. 3. The rapidity of the movement and organization of cav-1 during contraction was further studied by fluorescence recovery after photobleaching (FRAP). The recovery of fluorescence due to the movement of YFP-wt-cav-1 into an area of the membrane that contained fluorescence but has been rendered nonfluorescent via an intense photobleaching pulse of laser light was studied. The recovery of fluorescence after photobleaching as observed in *C–F* suggests that there is a dynamic movement of cav-1 that has been suggested to be characteristic of cav-1 to maintain the integrity of caveolae on the membrane. The recovery of fluorescence was much faster and enhanced in response to ACh stimulation as evident from the graph in *B*, suggesting that there is an increased dynamic movement of cav-1 upon ACh stimulation.
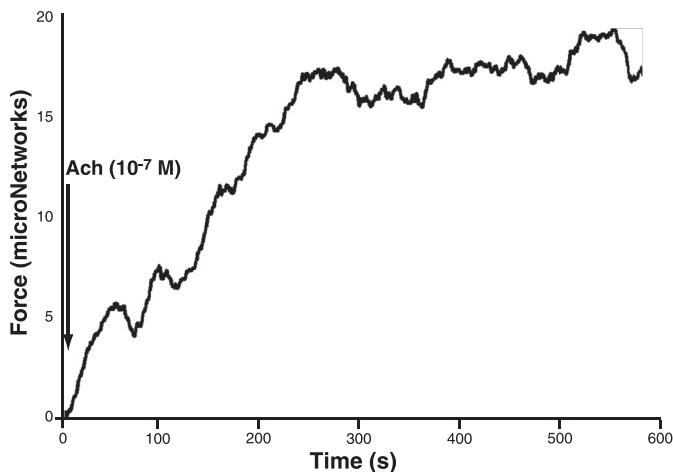
Fig. 4. Three-dimensional colonic circular smooth muscle rings were bioengineered from human CSMC. Colonic bioengineered rings were stretched ~50% and allowed to equilibrate before being stimulated with ACh (0.1 μM). An initial response was observed within 1 s of ACh addition. The force generated by human colonic bioengineered rings exhibited an initial rapid rise followed by sustained force generation.

factor in determining the cellular signaling (27). Expression of cav-1 is diminished in CSMC from aged rat. Cav-1 expression has also been seen to decline with age in Fischer 344 aortic vascular smooth muscle (43). Immunofluorescence analysis of cav-1 in CSMC from aged rat showed reduced fluorescence, indicating reduced amount of cav-1 protein compared with CSMC from adult rat (Fig. 5*A*). A reduction in cav-1 expression leading to diminished movement of cav-1 could impair cav-1 role as structural and functional protein. Transfection of CSMC from aged rat with YFP-wt-cav-1's cDNA showed increased fluorescence due to ectopic expression of the YFP-wt-cav-1 protein as observed by immunofluorescence analysis.

Contraction-associated organization of cav-1. In response to ACh stimulation, CSMC from adult rat showed shortening of cell length concomitant with preferential reorganization of cav-1 protein to the surface of the cell (Fig. 5*B*). Although CSMC from the aged rat showed reduced shortening of the cell length in response to ACh stimulation concomitant to its reduced expression of cav-1 proteins (Fig. 5*B*). Ectopic expression of YFP-wt-cav-1 in the CSMC from aged rat showed restoration of shortening of the cell length to the magnitude shown by CSMC from adult rat concomitant with redistribution of cav-1 protein to the surface (Fig. 5*B*). Furthermore, real-time monitoring of overexpressed cav-1 showed the dynamic movement of cav-1 along the organized cytoskeletal path similar to YFP-wt-cav-1 movement in human CSMC (Fig. 5*C*). Data suggest that ectopic expression of wt-cav-1 reinstates shortening of cell length, thus restoring the physiological contraction. Ectopic expression of wt-cav-1 may restore the dynamic movement and organization of cav-1. Restoration of dynamic movement of cav-1 could be responsible for the restoration of signaling pathways promoting the reinstatement of contractile response of aged rat CSMC.

Overexpressed cav-1 moves to membrane to form caveolae. Lipid raft membrane fractionation was performed to examine whether the overexpressed cav-1 moves to the membrane to form caveolae. Lipid raft membrane fractionation of aged rat CSMC untransfected and CSMC transfected with wt-cav-1

cDNA was performed. Twelve fractions from each sample were collected, and fractions 4 to 12 were run on SDS-PAGE followed by immunoblotted with anti-cav-1 antibody. In aged rat CSMC, untransfected, reduced levels of cav-1 proteins were observed in fractions 5–7, which are usually caveolin-enriched fractions in normal adult CSMC (47). Aged rat CSMC transfected with wt-cav-1 cDNA showed greatly enhanced levels of cav-1 in fractions 5–7 (Fig. 5*D*), similar to adult CSMC.

Mimicking aging: transfecting human CSMC with DN cav-1 cDNA. DN cav-1 cDNA is a cav-1/ΔTFT deletion mutation that has a 9-bp microdeletion corresponding to three amino acids: threonine-phenylalanine-threonine (amino acids 91–93) in the CSD of rabbit cav-1 cDNA. A mutation in CSD leads to impairment in caveolin structural and functional characteristics (33, 49). In human CSMC transfected with DN cav-1 (YFP-ΔTFT-cav-1) cDNA, fluorescence was observed in the cytosol close to the nucleus of the CSMC (Figs. 6*A* and 8). Biochemical analysis of human CSMC transfected with DN-cav-1 showed similarities to CSMC from aged rat with regard to contractile associated phosphorylation and interaction of contractile regulatory proteins (47). Real-time monitoring of these DN-cav-1 transfected CSMC did not show movement of fluorescent cav-1 in response to ACh (Fig. 6*B*). CSD is the protein domain responsible for some of the biological properties of cav-1. CSD is critical for caveolin homooligomerization and the interaction of caveolin with certain caveolin-associated proteins such as G proteins, H-Ras, and Src family kinases. ΔTFT deletion mutation in CSD attenuated the dynamic movement of cav-1 in CSMC transfected with DN cav-1 in response to ACh, leading to impairment in structural and functional activity of cav-1 protein and thus impairment of caveolae signal transduction functionality.

Percent cyclic movement of cav-1 in response to ACh. Dynamic cyclic movement of cav-1 was analyzed in rabbit CSMC transfected with either YFP-wt-cav-1 or with DN-cav-1 and in aged rat CSMC transfected with YFP-wt-cav-1. Human CSMC transfected with YFP-wt-cav-1 showed a significant increase in percent movement of cav-1 in response to ACh, which represents normal response to ACh. No significant movement of cav-1 in response to ACh was observed in human CSMC transfected with DN-cav-1, which mimic the response of aged CSMC to ACh. In aged rat CSMC transfected with wt-cav-1, there was significant restoration of the movement as evident by an increase in movement of cav-1 in response to ACh, similar to human CMSC transfected with YFP-wt-cav-1. The data were statistically developed by analyzing the region of interest using stack difference tool of ImageJ software. Calculating the mean of the movement of all the fluorescence particles and finding the difference between the mean movement before and after ACh stimulation gives us the value of real movement, which is then expressed as percentage. The graph representing the data suggest restoration of cav-1 dynamics in aged rat CSMC transfected with cav-1 (Fig. 7).

Force generation by colonic rings bioengineered from adult and aged rat CSMC. Colonic rings were bioengineered from adult and aged rats CSMC following the technique used to construct IAS three-dimensional bioengineered ring with slight modification (23). Bioengineered colonic rings were analyzed for force generation in response to ACh (Fig. 8*A*). Aged bioengineered colonic rings showed reduced generation of force in response to ACh compared with adult bioengineered
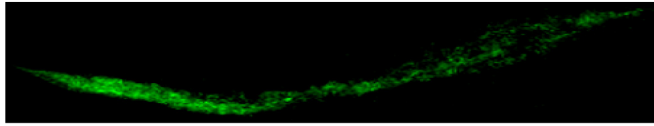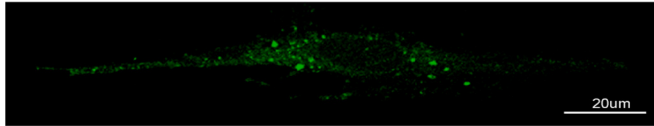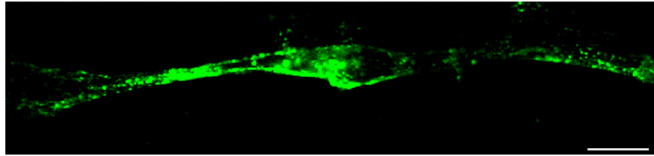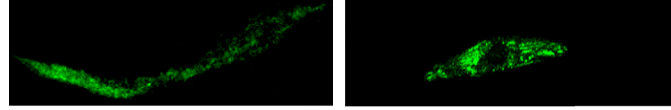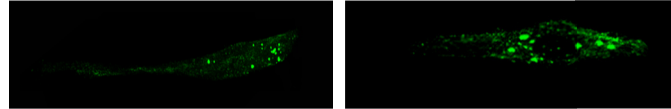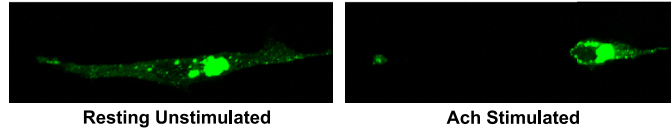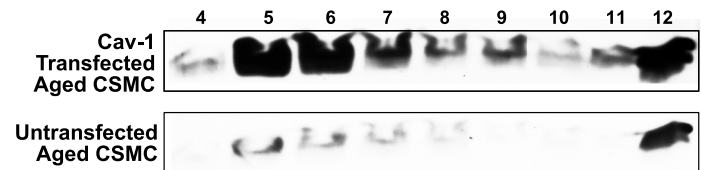
A Cav-1 Expression

Adult rat CSMC: Endogenous Caveolin Immunofluorescence

Aged rat CSMC: Endogenous Caveolin Immunofluorescence

20um

Aged rat CSMC: Transfected Caveoli-YFP Fluorescence

B Contraction of Adult/Aged Rat CSMC

CSMC from Adult Rat

CSMC from Aged Rat

YFP-Cav-1transfected CSMC from Aged Rat

Resting Unstimulated   Ach Stimulated

C Real-time Dynamic Movement of YFP-wt-Cav-1 in Transfected CSMC from Aged Rat
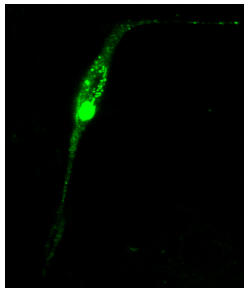
D Enrichment of over expressed caveolin in the lipid raft microdomains in Aged Rat CSMC transfected with YFP-wt-Cav-1

Cav-1 Transfected Aged CSMC

Untransfected Aged CSMC

4   5   6   7   8   9   10   11   12

Fig. 5. *A*: immunofluorescence analysis of aged rat CSMC showed reduced level of cav-1 compared with adult rat CSMC. Aged rat CSMC transfected with YFP-wt-cav-1 cDNA showed ectopic expression of YFP-cav-1 as observed by increased fluorescence. *B*: in response to ACh treatment, adult rat CSMC showed contraction with reorganization of cav-1 to the membrane and the distal cell surface, whereas CSMC from aged rat showed reduced contraction with reorganization of reduced amount of endogenous cav-1 present. However, aged rat CSMC transfected with YFP-wt-cav-1 showed contraction with reorganization of overexpressed cav-1. *C*: real-time monitoring of aged rat CSMC transfected with YFP-wt-cav-1 cDNA showed contraction similar to adult rat CSMC restoring the active, dynamic movement of cav-1. *D*: lipid raft membrane fractionation showed greatly enhanced levels of cav-1 in fractions 5–7 in aged CSMC overexpressing cav-1 compared with aged CSMC control. Fractions 5–7 are caveolin-enriched lipid raft fractions.

colonic rings (Fig. 8*A*). Colonic rings bioengineered from aged rat CSMC transfected with wt-cav-1 showed restoration of force generation (Fig. 8*B*). Ectopic expression of cav-1 was able to restore the force generation in colonic rings bioengineered from CSMC of aged rat similar to colonic rings bioengineered from CSMC of adult rat. Earlier studies have shown that cav-1 in caveolae modulate the contractile signal transduction pathway by its association with signaling molecules.

In summary, real-time monitoring of live human CSMC transfected with YFP-wt-cav-1 cDNA suggests that caveolin cycles within and along the membrane in a synchronized and highly organized pathways. These studies provide, for the first time, the advantage of the real-time monitoring of the dynamic movement of caveolin in living cells without fixing the cells. Thus rapid movement of cav-1 in response to ACh suggests that cav-1 plays a dynamic role in CSMC contraction. In line with previous studies, the present analysis suggests that cav-1 is essential for maintenance of caveolae on the membrane.

DISCUSSION

The emerging role of caveolae in organizing and modulating basic functions of smooth muscle presents the need to explore the dynamic role of its constituent protein cav-1 in smooth muscle function. Several studies using knockout mice have shown that, among the three isoforms of caveolin proteins, cav-1 is main component of the caveolar lipid raft microdomains on plasma membranes found in most cell types (4, 11, 26, 42, 52). Caveolae has been shown to play essential role in vascular smooth muscle function (26). Caveolae are organizational structure of central importance involved in increasingly complex system of signal transduction (4). Cav-1, caveolar structural protein, has been known as a scaffolding protein involved in localization and regulation of signaling molecules modulating signal transduction. Here, we examined the dynamic nature of cav-1 in colonic smooth muscle contraction by monitoring in real time live CSMC under confocal microscopy and by analyzing the force generated by bioengineered constructs in real time.
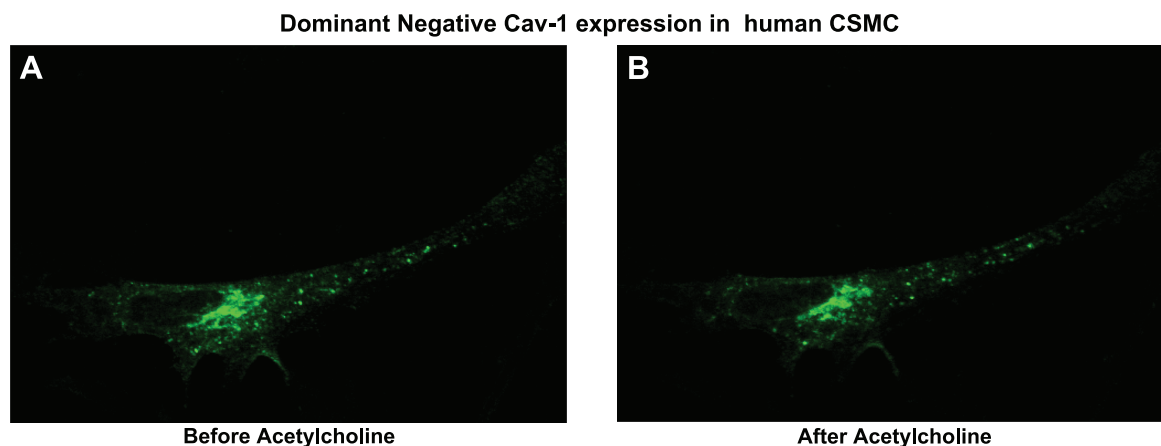
Dominant Negative Cav-1 expression in human CSMC

Before Acetylcholine

After Acetylcholine

Fig. 6. Human CSMC were transfected with dominant negative (DN) YFP-ΔTFT-cav-1 (TFT mutant: deletion of amino acids threonine-phenylalanine-threonine: 91–93 aa in the scaffolding domain). The dynamic movement of cav-1 observed in normal untransfected human CSMC was not observed in human CSMC transfected with DN cav-1. A reduced movement of cav-1 observed after ACh treatment suggests that functional cav-1 plays a crucial role in rapid cycling and dynamic movement of cav-1.

The phosphorylation of myosin light chain is the major event in initiation of contraction in smooth muscle (18). Upon contractile agonist stimulation, PKC-α and RhoA translocate and associate with cav-1 in the SMC membrane (47). Cav-1 expression is diminished in aged rat CSMC (47). Previous studies from our laboratory using biochemical assays have shown reinstatement of integrity of signal transduction pathways in CSMC from aged rats upon ectopic expression of cav-1 protein. Here, we demonstrate that ectopic expression of cav-1 restores the integrity of signaling pathways by restoration of cav-1 dynamics leading to restoration of caveolae functionality and thus physiological contractile response.
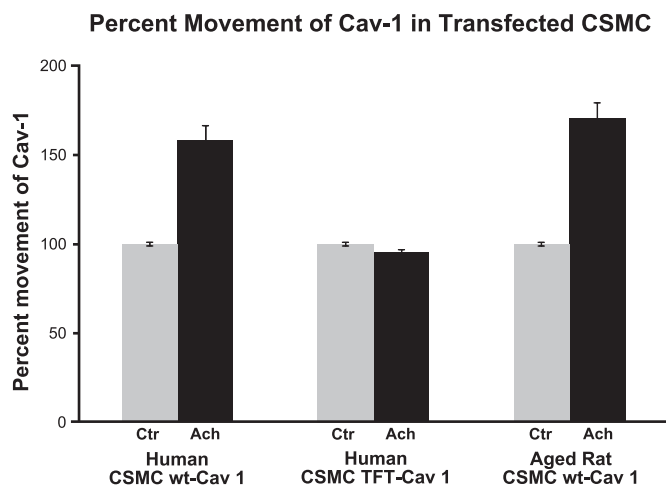
Percent Movement of Cav-1 in Transfected CSMC

Fig. 7. Dynamic and cyclic movement of cav-1 was statistically analyzed in human CSMC transfected with either YFP-wt-cav-1 or with DN-YFP-ΔTFT-cav-1 and in aged rat CSMC transfected with wt-cav-1. Human CSMC transfected with YFP-wt-cav-1 showed a significant increase in percent movement of cav-1 in response to ACh whereas no significant movement of cav-1 in response to ACh was observed in human CSMC transfected with DN-YFP-ΔTFT-cav-1. In aged rat CSMC transfected with wt-cav-1, there was significant increase in movement of cav-1 in response to ACh similar to human CMSC transfected with YFP-wt-cav-1. The graph representing the data suggest restoration of cav-1 dynamics in aged rat CSMC. Ctr, control.

In the present study, investigations were performed using either CSMC fixed on coverslip or on live CSMC grown on coverslip for real-time monitoring. CSMC from human were transfected with YFP-wt-cav-1 cDNA (Fig. 1). Cav-1 expression was characterized by an even cellular distribution with punctuate appearance in the fixed CSMC. Following ACh treatment, YFP-wt-cav-1 protein reorganized to the distal cell surfaces of SMCs indicating a dynamic movement of cav-1 in response to ACh (Fig. 1). Dynamic movement of cav-1 was monitored in real time in the human CSMC transfected with YFP-wt-cav-1 cDNA. A rapid cyclic movement of fluorescent cav-1 was observed on the membrane in response to ACh stimulation (Fig. 2) in human CSMC transfected with YFP-wt-cav-1 cDNA. The movement was synchronized and organized along the whole length of the cell characterized by rapid cycling of cav-1 along the membrane. Caveolae are regarded as one of the dynamic membrane microdomains that host many signaling events of different cellular processes (15, 20, 21, 26, 48, 51).

FRAP was used to track the real-time movement of cav-1 (Fig. 3) in SMCs of colon. Dynamic movement of cav-1 measured by the recovery of fluorescence showed a significant high percent recovery with fast mobility in the bleached section of the cells. The real-time movement of cav-1 was also tracked by FRAP in human CSMC stimulated with ACh, which showed that, in a given time, ACh-induced significantly high percent recovery compared with the unstimulated CSMC. This suggests that cav-1 movement is dynamic and movement was faster upon stimulation with ACh. Ectopic expression of DN-cav-1 in human CSMC significantly inhibited the mobility of cav-1 as no movement of cav-1 was observed in these cells with or without ACh (Fig. 4) similar to aged CSMC. DN-cav-1 mutant is a ΔTFT deletion mutation with a 9-base pair microdeletion that removes three amino acids (91–93) within the CSD (51). The expressed cav-1 is retained at the level of the Golgi complex in the perinuclear compartment and thus does not make it to the caveolae on the membrane. Mutation in CSD of cav-1 results in impairment in the interaction of cav-1 with many signaling molecules. Thus expression of DN-cav-1 may impair cav-1 functionality in smooth muscle, thereby impairing

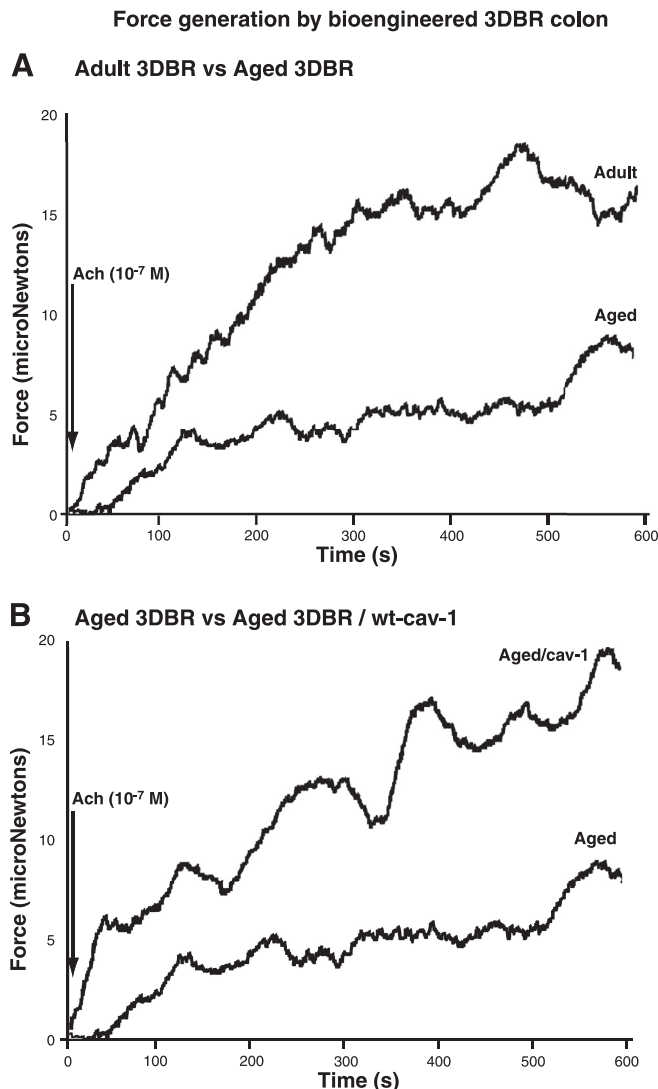**Force generation by bioengineered 3DBR colon**

Fig. 8. Colonic rings bioengineered from adult and aged rat CSMC were stretched and equilibrated in Krebs solution. Colonic rings bioengineered from adult rat CSMC exhibited initial rapid force generation followed by a substantial force generation in response to ACh (0.1 μM). Aging had an inhibitory effect on both initial rise and sustained phase of ACh-induced force generation as observed in colonic rings bioengineered from aged rat CSMC (*A*). Colonic rings bioengineered from aged rats CSMC transfected with wt-cav-1 coda showed restoration of physiological ACh-induced initial and sustained force generation (*B*). 3DBR, 3-dimensional bioengineered ring.

the contractile signal pathways or the dynamic movement of cav-1. This data suggest that levels of expression of functional cav-1 relates to the dynamic movement of cav-1.

CSMC from aged rat show decline in cav-1 expression and ectopic expression of wt-cav-1 in CSMC from aged rat restored the phosphorylation and association of contractile proteins pertinent to contraction in response to ACh (47). Similar observations were made with expression of cav-1 in endothelium to repair the vascular, cardiac, and pulmonary defects in global cav-1 knockout mice (34). Immunofluorescence analysis of cav-1 in fixed CSMC from aged rat showed reduced cav-1 confirming our earlier results (Fig. 5*A*). Here, we explored the real-time dynamic movement of cav-1 in CSMC from aged rat that ectopically expression YFP-wt-cav-1. Real-

time monitoring of live CSMC from aged rat transfected with YFP-wt-cav-1 showed reinstatement of cav-1 dynamics restoring the contraction (Fig. 5B, 5C, 7) as seen by percent cell length shortening of the CSMC in response to ACh. Observed increase in cyclic movement of cav-1 in aged CSMC overexpressing cav-1 corresponds to increase in cav-1 in their lipid raft membrane microdomain. This suggests that overexpressed cav-1 reinstates the caveolae and cav-1 functionality by restoring the dynamic, cyclic movement of cav-1. This is consistent with our earlier data showing restoration of ACh-induced decrease in cell length of CSMC from aged rat transfected with wt-cav-1 cDNA (47). Restoration of the dynamic movement and organization of cav-1 along the cytoskeletal path could be restoring the signaling pathways promoting the physiological contractile response of CSMC in aged rat.

Further studies were done to monitor the restoration of real-time force generation. Colonic rings were bioengineered by using CSMC from human and adult/aged rats. Colonic bioengineered rings from human CSMC showed physiological contractile response to ACh stimulation with initial response within 1 s. The force generated by human colonic bioengineered rings exhibited an initial rapid rise followed by sustained force generation (Fig. 4). Colonic bioengineered rings of aged rat CSMC showed reduced force generation in response to ACh compared with colonic bioengineered rings from adult rat (Fig. 8*A*). The force generated by colonic bioengineered rings from aged rat CSMC showed inhibition of initial rapid rise with reduction in the magnitude of force generation although the reduced force generated remained sustained. Data suggest that the signal transduction pathway related to cav-1 dynamics plays a more crucial role in the initial phase of contraction compared with later sustained phase of contraction. In ureteric muscle, it has been reported that cholesterol depletion affected phasic but not tonic contraction, suggesting that caveolae-related signaling regulates specific steps in excitation-contraction coupling (1).

DN-cav-1-transfected human CSMC showed inhibition of dynamic movement of cav-1 (Fig. 6). These CSMC mimicked the aged rat CSMC in inhibition of shortening of cell length potentially due to loss of integrity of signaling pathways correlating with inhibited cav-1 dynamic movement. Colonic bioengineered rings from aged rat CSMC transfected with wt-cav-1 cDNA showed restoration of force generation (Fig. 8*B*) with restoration of initial rapid rise and sustained phase of force generated. The data show that ectopic expression of cav-1 was able to restore the force generation in colonic bioengineered rings from CSMC of aged rat similar to colonic bioengineered rings from adult rat CSMC. Cav-1 in caveolae modulates the contractile signal transduction pathway by its association with signaling molecules (47). Aged rat CSMC with diminished cav-1 expression exhibited reduced association of cav-1 with signaling molecules which could be restored upon ectopic expression of cav-1 (47). These results indicate that cav-1 is an essential component of force generation in CSMC. Data give us insight into the mechanism of restoration of contraction in CSMC from aged rat upon ectopic expression of wt-cav-1. Restoration of contraction-related phosphorylation and association of proteins leading to restoration of force generation in CSMC from aged rat are essentially due to restoration of dynamics of cav-1. Initial events of CSMC contraction are influx of calcium,

which then forms calcium-calmodulin complex that activated MLCK, resulting in phosphorylation of MLC_{20} and thus initiation of contraction. Cav-1 is required for physiological calcium spark and regulation of transient calcium-activated potassium channels current in cerebral artery SMCs (11). Calcium influx in response to bethanechol was significantly reduced in the aged group compared with the young group, and it was concluded that the reduced contractile response to muscarinic stimulation of isolated urinary bladder strips from aged rats is mediated at least in part by a decreased rate of calcium entry (53). Data suggest that declined levels of cav-1 in aged rat CSMC abrogates contractile signal transduction due to impaired calcium influx essential for initiation of contraction. Ectopic expression of cav-1 in aged rat CSMC would restore cav-1 dynamic movement, thereby restoring the calcium influx resulting in reinstatement of contractile response. Restoration of cav-1 cycling dynamics reinstates the contractile signaling pathways regulating the contraction. The results further provide evidence for consideration of cav-1 as a possible therapeutic for age-related dysmotility or age-related sluggish colonic motility.

DISCLOSURES

No conflicts of interest, financial or otherwise, are declared by the author(s).

REFERENCES

1. **Babiychuk EB, Smith RD, Burdyga T, Babiychuk VS, Wray S, Draeger A.** Membrane cholesterol regulates smooth muscle phasic contraction. *J Membr Biol* 198: 95–101, 2004.
2. **Bender F, Montoya M, Monardes V, Leyton L, Quest AF.** Caveolae and caveolae-like membrane domains in cellular signaling and disease: identification of downstream targets for the tumor suppressor protein caveolin-1. *Biol Res* 35: 151–167, 2002.
3. **Bergdahl A, Gomez MF, Dreja K, Xu SZ, Adner M, Beech DJ, Broman J, Hellstrand P, Sward K.** Cholesterol depletion impairs vascular reactivity to endothelin-1 by reducing store-operated Ca^{2+} entry dependent on TRPC1. *Circ Res* 93: 839–847, 2003.
4. **Bergdahl A, Sward K.** Caveolae-associated signalling in smooth muscle. *Can J Physiol Pharmacol* 82: 289–299, 2004.
5. **Bhatnagar A, Sheffler DJ, Kroeze WK, Compton-Toth B, Roth BL.** Caveolin-1 interacts with 5-HT2A serotonin receptors and profoundly modulates the signaling of selected Galphaq-coupled protein receptors. *J Biol Chem* 279: 34614–34623, 2004.
6. **Biancani P, Walsh J, Behar J.** Vasoactive intestinal peptide: a neurotransmitter for relaxation of the rabbit internal anal sphincter. *Gastroenterology* 89: 867–874, 1985.
7. **Bitar KN.** Aging and Gi smooth muscle fecal incontinence: is bioengineering an option. *Exp Gerontol* 40: 643–649, 2005.
8. **Bitar KN, Hillemeier C, Biancani P, Balazovich KJ.** Regulation of smooth muscle contraction in rabbit internal anal sphincter by protein kinase C and Ins(1,4,5)P3. *Am J Physiol Gastrointest Liver Physiol* 260: G537–G542, 1991.
9. **Bitar KN, Patil SB.** Aging and gastrointestinal smooth muscle. *Mech Ageing Dev* 125: 907–910, 2004.
10. **Bonnevier J, Arner A.** Actions downstream of cyclic GMP/protein kinase G can reverse protein kinase C-mediated phosphorylation of CPI-17 and Ca^{2+} sensitization in smooth muscle. *J Biol Chem* 279: 28998–29003, 2004.
11. **Cheng X, Jaggar JH.** Genetic ablation of caveolin-1 modifies Ca^{2+} spark coupling in murine arterial smooth muscle cells. *Am J Physiol Heart Circ Physiol* 290: H2309–H2319, 2006.
12. **Couet J, Belanger MM, Roussel E, Drolet MC.** Cell biology of caveolae and caveolin. *Adv Drug Deliv Rev* 49: 223–235, 2001.
13. **Couet J, Sargiacomo M, Lisanti MP.** Interaction of a receptor tyrosine kinase, EGF-R, with caveolins. Caveolin binding negatively regulates tyrosine and serine/threonine kinase activities. *J Biol Chem* 272: 30429–30438, 1997.
14. **Dreja K, Voldstedlund M, Vinten J, Tranum-Jensen J, Hellstrand P, Sward K.** Cholesterol depletion disrupts caveolae and differentially impairs agonist-induced arterial contraction. *Arterioscler Thromb Vasc Biol* 22: 1267–1272, 2002.
15. **Dubroca C, Loyer X, Retailleau K, Loirand G, Pacaud P, Feron O, Balligand JL, Levy BI, Heymes C, Henrion D.** RhoA activation and interaction with Caveolin-1 are critical for pressure-induced myogenic tone in rat mesenteric resistance arteries. *Cardiovasc Res* 73: 190–197, 2007.
16. **Feron O, Han X, Kelly RA.** Muscarinic cholinergic signaling in cardiac myocytes: dynamic targeting of M2AChR to sarcolemmal caveolae and eNOS activation. *Life Sci* 64: 471–477, 1999.
17. **Fujita T, Toya Y, Iwatsubo K, Onda T, Kimura K, Umemura S, Ishikawa Y.** Accumulation of molecules involved in alpha1-adrenergic signal within caveolae: caveolin expression and the development of cardiac hypertrophy. *Cardiovasc Res* 51: 709–716, 2001.
18. **Gerthoffer WT, Murphey KA, Mangini J, Boman S, Lattanzio FA Jr.** Myosin phosphorylation and calcium in tonic and phasic contractions of colonic smooth muscle. *Am J Physiol Gastrointest Liver Physiol* 260: G958–G964, 1991.
19. **Glavind EB, Forman A, Madsen G, Tottrup A.** Effects of transmural field stimulation in isolated smooth muscle of human rectum and internal anal sphincter. *Am J Physiol Gastrointest Liver Physiol* 272: G1075–G1082, 1997.
20. **Gosens R, Stelmack GL, Dueck G, McNeill KD, Yamasaki A, Gerthoffer WT, Unruh H, Gounni AS, Zaagsma J, Halayko AJ.** Role of caveolin-1 in p42/p44 MAP kinase activation and proliferation of human airway smooth muscle. *Am J Physiol Lung Cell Mol Physiol* 291: L523–L534, 2006.
21. **Gosens R, Stelmack GL, Dueck G, Mutawe MM, Hinton M, McNeill KD, Paulson A, Dakshinamurti S, Gerthoffer WT, Thliveris JA, Unruh H, Zaagsma J, Halayko AJ.** Caveolae facilitate muscarinic receptor-mediated intracellular Ca^{2+} mobilization and contraction in airway smooth muscle. *Am J Physiol Lung Cell Mol Physiol* 293: L1406–L1418, 2007.
22. **Hartshorne DJ, Ito M, Erdodi F.** Myosin light chain phosphatase: subunit composition interactions and regulation. *J Muscle Res Cell Motil* 19: 325–341, 1998.
23. **Hecker L, Baar K, Dennis RG, Bitar KN.** Development of a three-dimensional physiological model of the internal anal sphincter bioengineered in vitro from isolated smooth muscle cells. *Am J Physiol Gastrointest Liver Physiol* 289: G188–G196, 2005.
24. **Hirano K, Derkach DN, Hirano M, Nishimura J, Kanaide H.** Protein kinase network in the regulation of phosphorylation and dephosphorylation of smooth muscle myosin light chain. *Mol Cell Biochem* 248: 105–114, 2003.
25. **Ito M, Nakano T, Erdodi F, Hartshorne DJ.** Myosin phosphatase: structure, regulation and function. *Mol Cell Biochem* 259: 197–209, 2004.
26. **Je HD, Gallant C, Leavis PC, Morgan KG.** Caveolin-1 regulates contractility in differentiated vascular smooth muscle. *Am J Physiol Heart Circ Physiol* 286: H91–H98, 2004.
27. **Kawabe JI, Grant BS, Yamamoto M, Schwencke C, Okumura S, Ishikawa Y.** Changes in caveolin subtype protein expression in aging rat organs. *Mol Cell Endocrinol* 176: 91–95, 2001.
28. **Kitazawa T, Takizawa N, Ikebe M, Eto M.** Reconstitution of protein kinase C-induced contractile Ca^{2+} sensitization in triton X-100-demembranated rabbit arterial smooth muscle. *J Physiol* 520: 139–152, 1999.
29. **Lasley RD, Narayan P, Uittenbogaard A, Smart EJ.** Activated cardiac adenosine A(1) receptors translocate out of caveolae. *J Biol Chem* 275: 4417–4421, 2000.
30. **Lisanti MP, Scherer PE, Vidugiriene J, Tang Z, Hermanowski-Vosatka A, Tu YH, Cook RF, Sargiacomo M.** Characterization of caveolin-rich membrane domains isolated from an endothelial-rich source: implications for human disease. *J Cell Biol* 126: 111–126, 1994.

31. **Lohn M, Furstenau M, Sagach V, Elger M, Schulze W, Luft FC, Haller H, Gollasch M.** Ignition of calcium sparks in arterial and cardiac muscle through caveolae. *Circ Res* 87: 1034–1039, 2000.

32. **Lopes GS, Ferreira AT, Oshiro ME, Vladimirova I, Jurkiewicz NH, Jurkiewicz A, Smaili SS.** Aging-related changes of intracellular Ca^{2+} stores and contractile response of intestinal smooth muscle. *Exp Gerontol* 2005.

33. **Martens JR, Sakamoto N, Sullivan SA, Grobaski TD, Tamkun MM.** Isoform-specific localization of voltage-gated K^+ channels to distinct lipid raft populations. Targeting of Kv15 to caveolae. *J Biol Chem* 276: 8409–8414, 2001.

34. **Murata T, Lin MI, Huang Y, Yu J, Bauer PM, Giordano FJ, Sessa WC.** Reexpression of caveolin-1 in endothelium rescues the vascular, cardiac, and pulmonary defects in global caveolin-1 knockout mice. *J Exp Med* 204: 2373–2382, 2007.

35. **Newton AC.** Protein kinase C: structure, function, regulation. *J Biol Chem* 270: 28495–28498, 1995.

36. **Oka N, Yamamoto M, Schwencke C, Kawabe J, Ebina T, Ohno S, Couet J, Lisanti MP, Ishikawa Y.** Caveolin interaction with protein kinase C. Isoenzyme-dependent regulation of kinase activity by the caveolin scaffolding domain peptide. *J Biol Chem* 272: 33416–33421, 1997.

37. **Okamoto T, Schlegel A, Scherer PE, Lisanti MP.** Caveolins, a family of scaffolding proteins for organizing "preassembled signaling complexes" at the plasma membrane. *J Biol Chem* 273: 5419–5422, 1998.

38. **Ostrom RS, Insel PA.** The evolving role of lipid rafts and caveolae in G protein-coupled receptor signaling: implications for molecular pharmacology. *Br J Pharmacol* 143: 235–245, 2004.

39. **Patil SB, Pawar MD, Bitar KN.** Phosphorylated HSP27 essential for acetylcholine-induced association of RhoA with PKCα. *Am J Physiol Gastrointest Liver Physiol* 286: G635–G644, 2004.

40. **Pike LJ, Casey L.** Localization and turnover of phosphatidylinositol 4,5-bisphosphate in caveolin-enriched membrane domains. *J Biol Chem* 271: 26453–26456, 1996.

41. **Quest AF, Leyton L, Parraga M.** Caveolins, caveolae, and lipid rafts in cellular transport, signaling, and disease. *Biochem Cell Biol* 82: 129–144, 2004.

42. **Razani B, Engelman JA, Wang XB, Schubert W, Zhang XL, Marks CB, Macaluso F, Russell RG, Li M, Pestell RG, Di Vizio D, Hou H Jr, Kneitz B, Lagaud G, Christ GJ, Edelmann W, Lisanti MP.** Caveolin-1 null mice are viable but show evidence of hyperproliferative and vascular abnormalities. *J Biol Chem* 276: 38121–38138, 2001.

43. **Schutzer WE, Reed JF, Mader SL.** Decline in caveolin-1 expression and scaffolding of G protein receptor kinase-2 with age in Fischer 344 aortic vascular smooth muscle. *Am J Physiol Heart Circ Physiol* 288: H2457–H2464, 2005.

44. **Shaul PW, Anderson RG.** Role of plasmalemmal caveolae in signal transduction. *Am J Physiol Lung Cell Mol Physiol* 275: L843–L851, 1998.

45. **Smart EJ, Graf GA, McNiven MA, Sessa WC, Engelman JA, Scherer PE, Okamoto T, Lisanti MP.** Caveolins, liquid-ordered domains, and signal transduction. *Mol Cell Biol* 19: 7289–7304, 1999.

46. **Somara S, Gilmont RR, Dennis RG, Bitar KN.** Bioengineered internal anal sphincter derived from isolated human internal anal sphincter smooth muscle cells. *Gastroenterology* 137: 53–61, 2009.

47. **Somara S, Gilmont RR, Martens JR, Bitar KN.** Ectopic expression of caveolin-1 restores physiological contractile response of aged colonic smooth muscle. *Am J Physiol Gastrointest Liver Physiol* 293: G240–G249, 2007.

48. **Tagawa A, Mezzacasa A, Hayer A, Longatti A, Pelkmans L, Helenius A.** Assembly and trafficking of caveolar domains in the cell: caveolae as stable, cargo-triggered, vesicular transporters. *J Cell Biol* 170: 769–779, 2005.

49. **Taggart MJ, Leavis P, Feron O, Morgan KG.** Inhibition of PKCalpha and rhoA translocation in differentiated smooth muscle by a caveolin scaffolding domain peptide. *Exp Cell Res* 258: 72–81, 2000.

50. **Tezuka A, Ishihata A, Aita T, Katano Y.** Aging-related alterations in the contractile responses to acetylcholine, muscarinic cholinoceptors and cholinesterase activities in jejunum and colon of the male Fischer 344 rats. *Exp Gerontol* 39: 91–100, 2004.

51. **Wertz JW, Bauer PM.** Caveolin-1 regulates BMPRII localization and signaling in vascular smooth muscle cells. *Biochem Biophys Res Commun* 375: 557–561, 2008.

52. **Woodman SE, Cheung MW, Tarr M, North AC, Schubert W, Lagaud G, Marks CB, Russell RG, Hassan GS, Factor SM, Christ GJ, Lisanti MP.** Urogenital alterations in aged male caveolin-1 knockout mice. *J Urol* 171: 950–957, 2004.

53. **Yu HI, Wein AJ, Levin RM.** Contractile responses and calcium mobilization induced by muscarinic agonists in the rat urinary bladder: effects of age. *Gen Pharmacol* 28: 623–628, 1997.